

The Numerical Simulation of Gas-Liquid Two Phase Flow in Annular Gap Venturi of Converter Wet Dust Removal

Mengmeng Ye, Mei Liang, Fuping Qian* and Jinli Lu

School of Civil Engineering and Architecture, Anhui University of Technology,
Ma'anshan 243002, China.

*Email: fpingqian@163.com

Abstract. Based on the CFD-DPM method, the numerical simulation of gas-liquid two phase flow in annular gap venturi with different annular gap trip and liquid/gas ratio at the same gas flow rate was carried out in this paper. The results show that the pressure drop at the contraction section of venturi accounts for about 75% of the total pressure drop, and the pressure drop at the throat is about 20% of the total pressure drop. The average velocity of flue gas at the throat ranges from 106 to 192m/s. The total pressure drop of the venturi is proportional to the liquid/gas ratio at the constant annular gap trip, and the larger the annular gap trip, the greater the effect of the liquid/gas ratio on the pressure drop. As the annular gap trip is 800~900mm, the effect of liquid/gas ratio on the pressure drop is significant. The total pressure drop of the venturi and the droplets concentration at the venturi inlet are proportional to the annular gap trip at the constant liquid/gas ratio, and the growth rate of the pressure drop is greater with the annular gap trip as the annular gap trip is larger than 700mm. In addition, the growth rate of the droplets concentration at the venturi outlet also increases with the annular gap trip.

1. Introduction

A large amount of gas is generated during the smelting in the converter, and due to much dust therein, it must be purified to be effectively utilized. OG (Oxygen Converter Gas Recovery) device is an important facility for converter gas recovery. The operation of ascensional annular gap venturi with adjustable throat directly affects the resistance and dust removal efficiency of the system. In recent years, many studies have been done on multiphase flow in venturi tube based on CFD method. Pak and Chang[1] used CFD software to conduct numerical simulation of gas-liquid-solid three phase flow in Pease - Anthony type venturi based on euler-lagrange method, and analyzed its pressure drop and dust removal efficiency. Lu Tao[2] et al. conducted three-dimensional numerical simulation of the flow and heat transfer process in the two-stage venturi of the third-generation OG system. Yu Xiaodong[3] carried out CFD simulation on the gas-liquid two phase complex flow problem of the descensional annular gap scrubber of the fourth generation OG system, revealing the characteristics of multi-phase flow field and the influence of various influencing factors on the resistance in the annular gap scrubber of the converter. Guerra [4] et al. studied the factors affecting the effect of liquid spraying through multiple orifices in venturi scrubber by experiments and CFD simulation; Sharifi[5] et al. accurately predicted the pressure drop in the venturi by combining the population balance equation with CFX. Zhang Xu [6] et al. used CFD software to calculate the mutual coupling between continuous phase flue gas and discrete phase water droplets in a diameter-adjustable venturi under actual working conditions. Most of the venturis in the above documents are of the descensional type, that is, the flue gas flows from top to bottom. In this paper, the ascensional type annular gap venturi with adjustable throat was studied, and the flue gas flows from bottom to top, and the scrubber cone is



ascentional. Compared with the venturi of previous generations of OG systems, it reduces system resistance and increases dust removal efficiency. Therefore, in-depth study and analysis of its internal multiphase flow are of great significance for optimizing the structure of the new OG system.

In this paper, the CFD-DPM method was used to numerically simulate the gas-liquid two phase flow in annular gap venturi. Under the same gas flow rate, the influence of different annular gap trip and different liquid/gas ratios on the pressure drop in the venturi and the droplet concentration at the venture outlet was analyzed. The obtained results have certain reference value for the optimal design of the annular gap venture in the new OG system.

2. Numerical Calculation Model of Annular Gap Venturi

2.1. Modeling and Meshing

Figure 1 shows a three-dimensional model of an annular gap venturi (the annular gap trip is 800 mm). The dust-containing gas enters from the bottom, and the middle part is a scrubber cone that can move up and down to adjust the opening rate of the venturi throat.

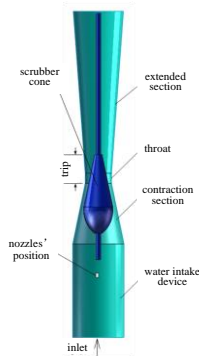


Figure 1. Annular gap venture



Figure 2. Mesh of the annular gap venture

Tetrahedral meshed by ICEM CFD, five mesh models with different annular trips were obtained. Figure 2 shows the mesh of the annular gap venturi with an annular gap trip of 800 mm. In order to improve the calculation accuracy, local encryption was used on the inlet and outlet of the annular gap venturi and the scrubber cone. Total number of grids: 314858, total number of nodes: 55786, grid quality: Min = 0.374, max = 0.999, average = 0.776.

2.2. Numerical Methodology

The furnace gas contains soot particles and flue gas. The soot particles mass concentration is about 4000 kg/m³, and the flue gas mass concentration 1.365 kg/m³; generally, dust mass concentration in the furnace gas is about 0.1 kg/m³, which shows that the volume occupied by the soot particles is much smaller than the volume of the flue gas, so the influence of the soot particles on the flow and heat transfer could be ignored [7]. Since the volume fraction of the spray droplets is much smaller than that of the flue gas, the flue gas is regarded as the continuous phase, and the spray droplets the discrete phase, and the two phases are coupled and calculated. The continuous phase adopts the Euler method to solve the NS equation. The continuous phase mathematical model includes the continuity equation, the momentum equation, the turbulent energy k equation, the turbulent dissipation ε equation and the energy equation. The discrete phase spray droplets adopt the Lagrangian particle orbit model.

The continuity equation, the momentum equation, and the energy equation can be expressed by a general formula [8]:

$$\frac{\partial(\rho\Phi)}{\partial t} + \nabla(\rho u\Phi) = \nabla(\Gamma \text{grad}\Phi) + S \quad (1)$$

Where Φ is a general variable, which can represent u , v , w , T and other dependent variables, Γ is a

generalized diffusion coefficient; S is a generalized source term. The four terms in the equation represent the transient term, the convection term, the diffusion term, and the source term respectively.

The Realizable k - ε model was selected as a turbulence model, and the turbulent energy k equation and the turbulent dissipation ε equation are as follows [9]:

$$\frac{\partial}{\partial t}(\rho k) + \frac{\partial}{\partial x_i}(\rho k u_i) = \frac{\partial}{\partial x_j} \left[\left(\mu + \frac{\mu_t}{\sigma_k} \right) \frac{\partial k}{\partial x_j} \right] + G_k + G_b - \rho \varepsilon - Y_M + S_k \quad (2)$$

$$\frac{\partial}{\partial t}(\rho \varepsilon) + \frac{\partial}{\partial x_i}(\rho \varepsilon u_i) = \frac{\partial}{\partial x_j} \left[\left(\mu + \frac{\mu}{\sigma_\varepsilon} \right) \frac{\partial \varepsilon}{\partial x_j} \right] + C_{1\varepsilon} \frac{\varepsilon}{k} (G_k + C_{3\varepsilon} G_b) - C_{2\varepsilon} \rho \frac{\varepsilon^2}{k} + S_\varepsilon \quad (3)$$

Where G_k and G_b represent the turbulent flow energy produced by the laminar velocity gradient and the buoyancy force, respectively. Y_M is the wave effect generated by transitional diffusion in compressible flow. $C_{1\varepsilon}$, $C_{2\varepsilon}$, $C_{3\varepsilon}$ are constant, and σ_k and σ_ε are the turbulent Prandtl numbers in the k and ε equations, and S_k and S_ε are user-defined values.

The motion equation of the droplet:

$$\frac{du_p}{dt} = F_d(u - u_p) + \frac{g(\rho_p - \rho)}{\rho_p} + F \quad (4)$$

Where $F_d(u - u_p)$ is the unit mass drag force of the flue gas on the droplets (in this paper, spherical law is used, i.e. the droplet is assumed to be spherical particle).

$$F_d = \frac{18\mu}{\rho_p d_p^2} \frac{C_d Re_p}{24} \quad (5)$$

Where u_p , g , u , ρ_p , F , C_d and Re_p are the droplet velocity, gravitational acceleration, droplet density, additional mass force (ignored herein), drag coefficient, and droplet relative Reynolds number.

Within the same time step, the equation was resolved by the SIMPLE algorithm. The pressure, momentum, turbulent kinetic energy and turbulent diffusivity are all in the second-order upwind discrete scheme. On the basis of the first-order upwind discrete scheme, this format considers the influence of the curvature of the curve about the distribution of physical quantities among nodes, which helps to improve the accuracy and stability of the calculation. The residual convergence criterion for continuity, velocity, turbulent kinetic energy, and turbulent diffusivity are all set to 0.001.

For the discrete phase, in order to accurately describe the spraying process, the gravity, drag force and droplets breakage are considered in the simulation calculation. Taking the droplet group as a discrete system, the orbit of the discrete phase particles is obtained by differential equation of particle force in integral Lagrangian coordinate system. The droplets are tracked by an unsteady discrete phase model [10], and random orbital model is used to consider the turbulent diffusion of the particles. The random walk model in the tracking model of the particles is used to consider the interaction between the particles and the discrete vortices of the fluid.

2.3. Boundary Conditions

The external atmospheric pressure is 101325 Pa. The flue gas rate at the Venturi inlet is 105 000 m³/h, and the venturi nozzle with forward spray mode is located on the central axis of the water intake device. The specific simulation settings are shown in Table 1 and Table 2.

Table 1. Continuous phase boundary conditions

Items	Continuous phase boundary conditions
Inlet boundary type	Velocity-inlet
Inlet Velocity	18.96m/s
OutletBoundary Type	Pressure-outlet.
Outlet Pressure	0
Turbulent Intensity	5%
Turbulence Viscosity Ratio	10
Wall Boundary Type	No-slip Wall; Adiabatic; Particle Escape
Inlet and Outlet Temperature	300K

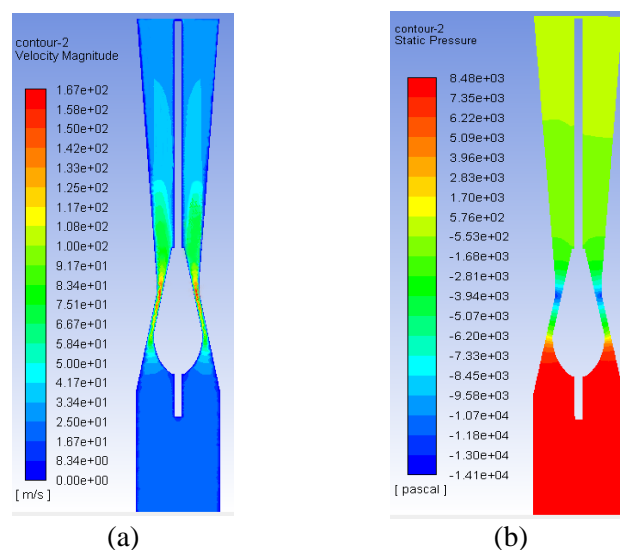
Table 2. Discrete phase model settings

Items	DPM settings
Nozzle Type	Pressure Swirling Nozzle
Droplet Type	Droplet
Water Temperature	300K
Pressure	1MPa
Nozzle Diameter	5mm

3. Numerical Simulation Results and Analysis

3.1. Flow Field Distribution

The velocity and pressure contour on the symmetrical plane of Venturi with different annular gap trips were obtained by numerical simulation, as shown in Figure 3 (taking 800mm annular gap trip as an example). As can be seen from Figure 3, in general, the pressure drops at the contraction section, where the pressure drop accounts for about 75% of the total pressure drop. The pressure drop at the throat is about 20% of the total pressure drop. The pressure value reaches a minimum at the throat and partially builds up in the extended section. This is because as the cross-section area of the shrinkage section decreases, the flue gas velocity increases. The flue gas velocity at the throat is accelerated to its maximum value. The static pressure decreases with the increase of flue gas velocity. Then the flow velocity decreases gradually with the increasing cross-section area of the expansion section, and the static pressure rises to a certain extent. The average flue gas velocity at the throat reaches 106-192 m/s in the range of annular gap trips selected in this paper.

**Figure 3.** Velocity and pressure contours of annular gap venturi

3.2. Effect of the Annular Gap Trip on Average Throat Velocity and Droplet Concentration at Venturi Outlet

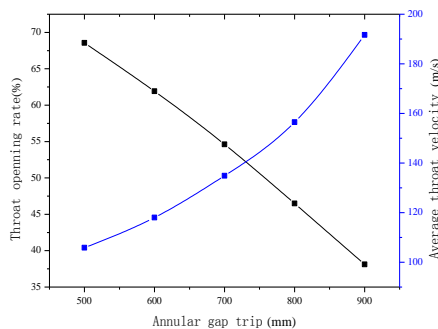


Figure 4. The variation of throat opening rate and average throat velocity versus the annular gap trip

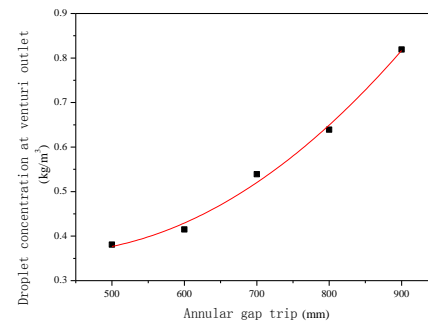


Figure 5. The variation of the droplet concentration at the venturi outlet versus the annular gap trip

It can be seen from Figure 4 that the throat opening rate decreases almost linearly with the increase of the annular gap trip, and the average throat velocity gradually increases with the increase of the annular gap trip. However, since the gas is compressible, the resistance or pressure of the flue gas vary with different annular gap trip, and as the annular gap trip increases, the flue gas velocity at the throat turns larger, and the impact of the gas on the water is more intense. Therefore, the flue gas velocity at the throat does not vary linearly with the annular gap trip.

Figure 5 shows the variation of the droplet concentration at the venturi outlet versus the annular gap trip when the gas flow rate and the liquid/gas ratio are constant. It can be seen from Figure 5 that, in general, the droplet concentration at the venturi outlet increases as the annular gap trip increases, and growth rate of the droplet concentration at the venturi outlet also increases as the annular stroke increases. This is because, as the annular gap trip increases, the throat gas velocity gradually increases (as shown in Figure 4). The droplet breakage mainly occurs at the throat. The larger the throat gas velocity, the better the droplet breakage effect. Therefore, the droplet concentration at the venturi outlet increases as the annular gap trip increases. When the water spray flow rate is constant, the higher the outlet droplet concentration, the larger the specific surface area of the droplet, which helps dust particles to be encapsulated by droplets and improves dust removal efficiency of the system.

3.3. Effect of the Annular Gap Trip and Liquid/Gas ratio on Pressure Drop

Figure 6 shows the variation of the total pressure drop of annular venturi versus annular gap trip under constant gas velocity and different liquid/gas ratio.

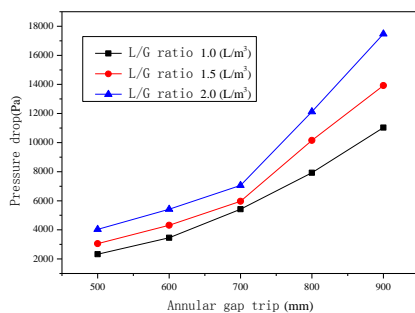


Figure 6. The variation of pressure drop versus annular gap trip

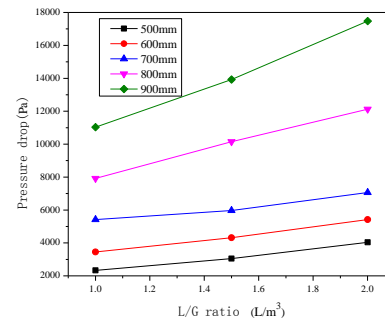


Figure 7. The variation of pressure drop versus liquid/gas ratio

Figure 6 shows that the pressure drop of the annular gap venturi increases with the increase of the annular gap trip at the constant liquid/gas ratio. The growth rate of the pressure drop is greater with the

annular gap trip as the annular gap trip is larger than 700mm. This is because when the annular gap trip is larger than 700 mm, the average flow velocity at the throat increases rapidly (as shown in Figure 4), so the pressure decreases greatly at the throat, and the increase of total pressure drop with the increase of annular gap trip is also more significant. In addition, at the constant annular gap trip, the larger the liquid/gas ratio, the greater the pressure drop of the annular gap venturi. This is because with the increase of the liquid/gas ratio, the energy consumption of gas for accelerating droplets increases. The resistance in the annular gap increases, that is, the pressure drop of the scrubber increases.

Figure 7 shows the variation of pressure drop versus liquid/gas ratio at the constant gas flow rate and different annular gap trip. As shown in Figure 7, the larger the annular gap trip, the greater the effect of liquid/gas ratio on pressure drop. When the annular gap trip is larger than 800mm, the effect of liquid/gas ratio on pressure drop is more significant. When the liquid/gas ratio is 2.0 L/m^3 , the pressure drop under the maximum annular gap trip has exceeded 17 kPa. Therefore, it is suggested that the liquid/gas ratio be controlled below 2.0 L/m^3 .

4. Conclusions

Based on CFD-DPM method, the numerical simulation of gas-liquid two-phase flow in annular gap venturi in new OG system was carried out. The effect of different annular gap trip and liquid/gas ratio on the pressure drop of venturi and droplet concentration at venturi outlet under the constant gas flow rate was analyzed. The conclusions are as follow:

(1) The pressure drop increases greatly at the contraction section, the pressure drop at the contraction section accounts for about 75% of the total pressure drop, and the pressure drop at the throat accounts for about 20% of it. The pressure reaches a minimum at the throat and the partially builds up during the extended section. The gas velocity is accelerated to its maximum value at the throat. As the annular gap trip is 500~900mm, the average flow velocity at the throat ranges from 106 to 192m/s.

(2) At the constant gas flow rate and annular gap trip, the pressure drop of annular gap venturi is proportional to the liquid/gas ratio. The larger the annular gap trip, the greater the effect of liquid/gas ratio on the pressure drop. Especially when the annular gap trip is larger than 800mm, the influence of liquid/gas ratio on pressure drop is more significant. Therefore, it is suggested that the liquid/gas ratio be controlled below 2.0 L/m^3 .

(3) Under the constant gas flow rate and liquid/gas ratio, the pressure drop of the annular gap venturi is proportional to the annular gap trip, and the pressure drop increases greatly when the annular gap trip is larger than 700 mm; the droplet concentration at the venturi outlet is proportional to the annular gap trip, and the growth rate of the droplet concentration at the outlet also increases with the annular gap trip. When the annular gap trip is larger than 700 mm, the droplet concentration at the venturi outlet increases greatly, which is more conducive to improving the dust removal efficiency of the system, however, the pressure drop of venturi increases greatly with the annular gap trip, and excessive pressure drop will reduce the service life of the system equipment.

5. Acknowledgement

This study was financially supported by Provincial Major Project of Natural Science Research for Colleges and Universities of Anhui Province (grant no. KJ2017ZD06).

6. References

- [1] Pak S I and Chang K S. Performance estimation of a venturi scrubber using a computational model for capturing dust particles with liquid spray [J]. *Journal of Hazardous Materials*, 2006, **vol5 no105**, pp560-573.
- [2] Lu T and Liu C G. Influence of gas rate, spraying rate, and opening rate on performance of flow and heat transfer in venturi tube for converter gas [J]. *Journal of Thermal Science and Technology*, 2007, **vol6 no4**, pp309-312.
- [3] Yu X D. Research on the pressure drop characteristics of multiphase flow in the ring silt washer of converter gas [D]. Chongqing University, 2008.
- [4] Guerra V G, Goncalves J A S and Coury J R. Experimental investigation on the effect of liquid

- injection by multiple orifices in the formation of droplets in a venture scrubber[J]. *Hazardous Materials*, 2009, **vol161 no1**, p 351.
- [5] Sharifi A and Mohebbi A. A combined CFD modeling with population balance equation to predict pressure drop in venturi scrubbers [J]. *Research on Chemical Intermediates*, 2014, **vol40 no3**, pp1021-1042.
- [6] Zhang X, Wang H J, Wu S F et al. Optimization of venturi tube gas-liquid coupling numerical simulation[J]. *Metallurgical Equipment*, 2014, no212, pp 54~57.
- [7] Lu T and Huang C. Performance analysis of flow and heat transfer of spraying cooling for converter gas with high temperature in venturi tube [J]. *Journal of Thermal Science and Technology*, 2007, **vol6 no1**, p33.
- [8] Zhang J Q. Calculation of performance of oxygen converter gas wet purification system and simulation of flow and heat transfer of a venture scrubber [D]. Beijing University of Chemical Technology: College of Mechanical Engineering, 2015.
- [9] Zhang X. The converter flue gas purification and recycling system optimization and engineering practice [D]. Yanshan University: College of Mechanical Engineering, 2012.
- [10] Han Z Z, Wang J and Lan X P. FLUENT: Example and Analysis of Fluid Engineering Simulation [M]. Beijing: Beijing Institute of Technology Press, 2004, pp5-44.